
Inevitable Encounters: Backdoor Attacks Involving Lossy Compression

Qian Li^{1,2} Yunuo Chen¹ Yuntian Chen^{2*}

¹Shanghai Jiao Tong University ²Eastern Institute of Technology

Abstract

Real-world backdoor attacks often require poisoned datasets to be stored and transmitted before being used to compromise deep learning systems. However, in the era of big data, the inevitable use of lossy compression poses a fundamental challenge to invisible backdoor attacks. We find that triggers embedded in RGB images often become ineffective after the images are lossily compressed into binary bitstreams (e.g., JPEG files) for storage and transmission. As a result, the poisoned data lose its malicious effect after compression, causing backdoor injection to fail. In this paper, we highlight the necessity of explicitly accounting for the lossy compression process in backdoor attacks. This requires attackers to ensure that the transmitted binary bitstreams preserve malicious trigger information, so that effective triggers can be recovered in the decompressed data. Building on the region-of-interest (ROI) coding mechanism in image compression, we propose two poisoning strategies tailored to inevitable lossy compression. First, we introduce Universal Attack Activation, a universal method that uses sample-specific ROI masks to reactivate trigger information in binary bitstreams for learned image compression (LIC). Second, we present Compression-Adapted Attack, a new attack strategy that employs customized ROI masks to encode trigger information into binary bitstreams and is applicable to both traditional codecs and LIC. Extensive experiments demonstrate the effectiveness of both strategies.

1 Introduction

In recent years, the widespread use of deep learning has increased vulnerability to security threats [1, 2, 3, 4, 5, 6, 7, 8, 9, 10, 11, 12, 13]. One significant threat is data poisoning-based backdoor attacks, where adversaries inject malicious “triggers” into datasets and release them for users to download and train their models [14, 15, 16, 17, 18]. The trained models perform normally on clean samples, but exhibit specific attacker-controlled behaviors when triggered. Such attacks are covert and difficult to detect, posing serious threats to the security and reliability of machine learning systems.

With the rapid growth of data volume and increasing network transmission demands, the storage and transmission of massive data now rely more on efficient and cost-effective lossy image compression methods [19, 20, 21]. However, the increasingly inevitable use of lossy compression poses a challenge to many existing backdoor attacks. Since these methods typically add triggers directly to RGB images $\mathbf{x}_p = \mathbf{x} + \delta \in \mathbb{R}^{3 \times H \times W}$, they do not ensure that the poisoned sample \mathbf{x}_p retains effective trigger information after lossy compression into binary bitstream file $\hat{\mathbf{y}} \in \{0, 1\}^n$ (such as .jpeg format files using JPEG), nor that the decompressed RGB images $\hat{\mathbf{x}}_p \in \mathbb{R}^{3 \times H \times W}$ recovered from $\hat{\mathbf{y}}$ still contain effective trigger. In practice, lossy compression introduces distortion ($\hat{\mathbf{x}} \neq \mathbf{x}$) and can destroy or attenuate trigger signals, omitting this step renders current mainstream backdoor attacks ineffective, including invisible trigger methods and clean-label attacks [22, 23, 24, 25, 26, 27]. As shown in the left of Fig. 1, the toxicity of poisoned datasets by previous invisible attacks diminishes

*Corresponding Author

after the lossy compression, leading to the failure of injecting backdoors into the trained models. Inspired by previous works [28, 29], we suggest that this ineffectiveness arises because invisible triggers often alter or introduce high-frequency components. The right panel of Fig. 1 shows that these high-frequency components are crucial for the triggers. Even though these triggers achieve stealth by hiding in the high-frequency components, they are sensitive to compression. During the lossy compression, the severe distortion of the trigger’s high-frequency components compromises its integrity, rendering the attack ineffective.

In this paper, we emphasize the importance of considering lossy compression’s impact on backdoor attacks as data volumes grow. This requires attackers to ensure that both the transmitted bitstream and the decompressed data carry malicious trigger information, rather than merely adding and testing the toxicity of the raw RGB data x . We implement backdoor attacks involving lossy compression by utilizing the ROI (Region of Interest) functionality [30, 31, 32, 33, 34], which is a common optional functionality in the data compression literature. ROI functionality can guide codecs to assign different bitrates to various regions of an image, thereby controlling the compression distortion in each area. Based on the ROI, we propose two backdoor attacks under lossy compression that target emerging learned image compression (LIC) [35, 36, 37, 38] and widely used traditional codecs: 1. We propose a Universal Attack Activation method for LIC to reactivate invisible triggers from previous works that fail under lossy compression. A sample-specific ROI mask is designed to allocate more bitrate to high-frequency regions of the triggers, mitigating compression-induced distortion on the trigger integrity and protecting the trigger information in the binary bitstream \hat{y} . Consequently, the decompressed poisoned data retains valid triggers. 2. We propose a novel, invisible, and Compression-Adapted backdoor Attack, named CAA, for both LIC and traditional codecs. A customized ROI mask is designed to embed trigger information into the binary bitstream \hat{y} . This mask produces the transmitted data to exhibit a special high-frequency distribution pattern that is invisible and can serve as a trigger. Extensive experiments show the effectiveness of two methods.

Our contributions are summarized as follows.

- We reveal that previously effective invisible triggers, including those used in clean-label attacks, often fail under lossy data compression. This finding highlights the necessity of accounting for the inevitable lossy compression process in data poisoning.
- We propose a Universal Attack Activation method for LICs to restore the effectiveness of invisible triggers degraded by lossy compression. Extensive experiments demonstrate that the proposed method significantly improves the attack success rates of prior attacks under lossy compression while maintaining strong invisibility.
- A novel invisible attack CAA is proposed for both LICs and traditional codecs that adapts to lossy compression. Extensive experiments demonstrate that CAA achieves outstanding attack success rates and superior invisibility under lossy compression.

2 Related Work

2.1 Invisible Backdoor Attack

Gu *et al.* first introduced a backdoor attack by their BadNets proposal [8], which has sparked a lot of research interest on backdoor attack [39, 12, 40, 41]. Recently, researchers have increasingly focused on the invisibility of backdoor triggers to develop more powerful attacks. ISSBA [42] embedded class-specific strings into images using pre-trained networks and image steganography

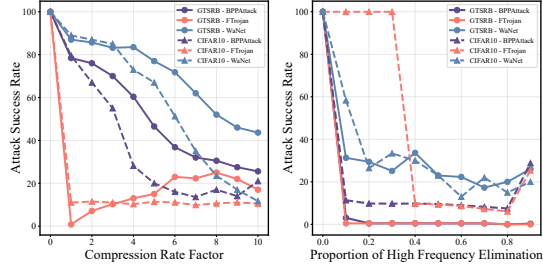


Figure 1: **Ineffectiveness of Backdoor Attacks.** **Left:** Higher compression rates intensify image distortion, hindering backdoor injection. It suggests that compression severely damages invisible triggers. **Right:** Removing high-frequency components from poisoned test samples via Fast Fourier transform significantly lowers the ASR, highlighting their crucial role in invisible triggers.

techniques. WaNet [24] applied image warping as triggers, making the modifications difficult for humans to notice. Besides, BppAttack [22] took advantage of vulnerabilities in the human visual system, reducing visible changes through image quantization and improving trigger accuracy with contrastive learning. FTrojan [23] used perturbations in the frequency domain, spreading subtle pixel-wise changes throughout the image. Additionally, Rao *et al.* [29] proposed a backdoor attack method based on semantic information in the frequency domain.

Clean-label attack [26, 27, 43, 44] is a special type of invisible backdoor attack that implants a backdoor without altering sample labels, enabling stealthier data poisoning. Its triggers are typically tiny, high-frequency adversarial perturbations and are therefore especially vulnerable to distortion from lossy compression.

However, existing invisible backdoors overlook lossy compression effects, which remove high-frequency trigger components and degrade attack performance.

2.2 Lossy Image Compression

Lossy image compression aims to reduce image storage and transmission costs by removing perceptually redundant information while maintaining visually acceptable quality. As image data volumes surge, lossy image compression is increasingly vital for efficient data storage and transmission.

Traditional compression methods, such as JPEG, JPEG2000, and BPG, rely heavily on hand-crafted transforms combined with entropy coding. These methods benefit from decades of optimization and standardization, offering stable performance. Recent advances in Learned Image Compression (LIC) models have surpassed traditional codecs in rate-distortion performance, enhancing image storage and transfer capabilities significantly. Ballé *et al.* [45] introduced the first end-to-end LIC model using convolutional neural networks (CNN). Later, they developed a variational auto-encoder (VAE) based compression model enhanced with a hyper-prior [46], establishing a foundational framework for modern learned image compression models. More recent studies have proposed sophisticated transform networks [47, 48, 49, 50, 51, 52] and advanced entropy models [53, 54, 55, 56], showcasing the constant development in this field.

Thus, lossy data compression has become inevitable in modern data poisoning pipelines, and ignoring it may render existing methods ineffective in real-world applications.

3 Backdoor Attacks under Lossy Compression

The first column of Fig. 2 shows the process of a data poisoning based backdoor attack. Attackers (senders) use an encoder (e.g., the encoder of JPEG codec) to compress all RGB raw images $\{\mathbf{x} \in \mathbb{R}^{3 \times H \times W}\}_{i=1}^N$ (both poisoned and benign) into binary bitstream format files $\{\hat{\mathbf{y}} \in \{0, 1\}^n\}_{i=1}^N$ (e.g., .jpeg files) while storing. The process can be expressed as form 1, where Q is a quantization operator and $\hat{\mathbf{y}}$ is the binary bitstream with the compression format of Encoder used. The binary bitstream data $\hat{\mathbf{y}}$ will be transmitted to victims. When victims (receivers) need access data for training or other tasks, the system automatically invokes the built-in Decoder matching to the Encoder used, by the file extension (e.g., files with .jpeg extension will automatically invoke the JPEG decoder when accessing data). The decompression process transforms the bitstream $\hat{\mathbf{y}}$ to the RGB image $\hat{\mathbf{x}}$, as shown in the form 2. DeQ is a dequantization operator that acts as an identity mapping in LIC. Previous methods overlooked compression distortion in the " $\mathbf{x} \rightarrow \hat{\mathbf{y}}$ " process, which results in the bitstream $\hat{\mathbf{y}}_p$ of poisoned data \mathbf{x}_p lacking effective trigger information and the decompressed poisoned data $\hat{\mathbf{x}}_p$ is benign. Thus, the invisible triggers failed in real-world applications with lossy compression.

$$\text{Compression : } \hat{\mathbf{y}} = \text{Q}(\text{Encoder}(\mathbf{x})); \quad (1)$$

$$\text{Decompression : } \hat{\mathbf{x}} = \text{Decoder}(\text{DeQ}(\hat{\mathbf{y}})). \quad (2)$$

We reassess the attacker’s targets, capabilities, and constraints as follows:

Targets: 1. Models trained on decompressed poisoned datasets successfully embed backdoors while accurately classifying decompressed benign samples. 2. $\hat{\mathbf{y}}_p$ with trigger information can be decompressed normally by the built-in decoder. 3. The triggers in the decompressed poisoned data $\hat{\mathbf{x}}_p$ remain invisible.

Capabilities: Since the models and parameters of standard paired codecs are publicly available,

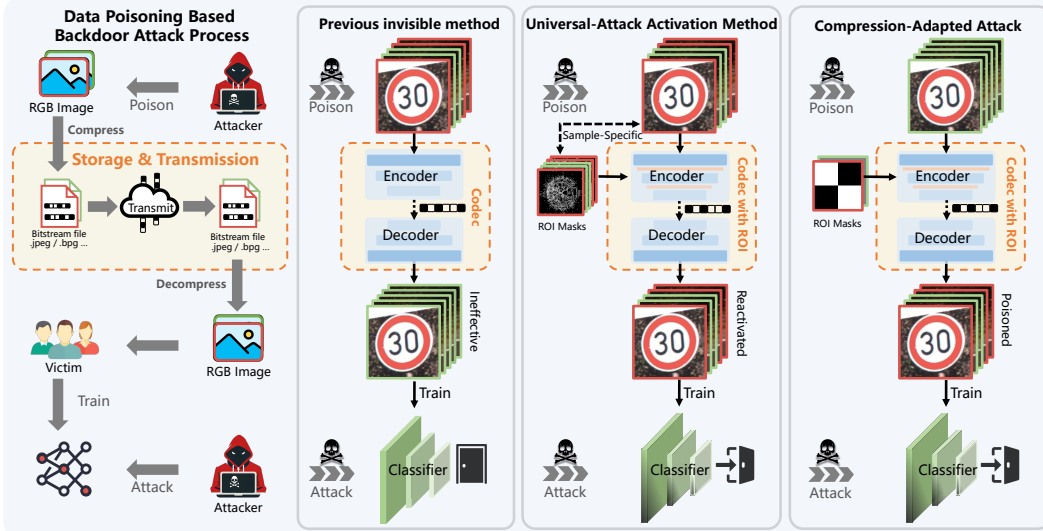


Figure 2: **Overview.** Red borders indicate poisoned samples, While green borders indicate benign samples. **The first column** outlines the process of data poisoning, which contains the inevitable compression process. **The second column** describes that the previously invisible method fails in real-world scenarios. We propose two methods described in the third and fourth columns: **1. Universal Attack Activation Method:** It is a general method that reactivates methods previously ineffective under lossy compression. This method is particularly suitable for LICs and a few traditional codecs that support pixel-level ROI functionality. **2. Compression-Adapted Attack:** It is a novel compression-adapted attack method that is applicable to most codecs.

attackers can design attacks leveraging the codec’s information.

Constraints: 1. Attackers cannot interfere with the decompression process, as they cannot compel victims to use a specially modified decoder. 2. Attacks must ensure normal compression and decompression, meaning: (a) the total bit rate of images is normal. (b) the decoding time is normal, (c) the invoking of the decoder is normal (the bitstream format remains intact), and (d) the decompressed image appears normal.

3.1 Codecs with ROI support

To ensure normal compression and decompression, the codec must remain pure. Therefore, we use a commonly employed functionality in image compression called Region of Interest (ROI), rather than introducing any additional backdoor modules. The codec with ROI takes a manually adjustable ROI mask as input, which specifies different weights for each region in the image. Specifically, the compression process can be described as form 3, where $\mathbf{M} = [m_{i,j}] \in \mathbb{R}^{H \times W}$ is the ROI mask. $m_{i,j}$ represents the bitrate allocation weight of the pixel at the i -th row, j -th column. The higher the weight, the more bitrate is allocated to the corresponding pixel, resulting in less distortion.

$$\text{Compression} : \hat{y} = Q(\text{Encoder}(x, \mathbf{M})). \quad (3)$$

Numerous studies have integrated ROI functionality into both traditional codecs and LIC models [57, 58, 30, 59, 31, 32], enabling us to directly leverage publicly available codecs for data poisoning in a manner consistent with the aforementioned **Capabilities**. To provide practical insights into data poisoning under lossy compression, we propose two ROI-based methods following distinct technical routes. The method in Sec. 3.2 applies to LICs with pixel-level ROI support, while the method in Sec. 3.3 targets codecs with region-level ROI support, covering both traditional codecs and LICs.

In particular, since integrating ROI functionality into LICs is straightforward, attacks targeting LICs are easier to implement. We briefly introduce a general method for integrating ROI into LIC, providing background guidance for future research on attacks and defenses in this setting. We can follow Song *et al.* [31] to introduce the Spatial Feature Transform (SFT) module to integrate ROI, which can be integrated into any LIC model. SFT module provides an interface for receiving a ROI mask \mathbf{M} . In our backdoor attack context, to comply with the **Constraints**, the SFT module can only be inserted in the encoder, and is trained on the clean datasets of image compression

while other parameters of codecs are frozen. For traditional codecs, we can directly refer to prior works [57, 58, 60] and leverage ROI to implement the attack.

Next, we provide two ROI-based attack strategies in the lossy compression scenario.

3.2 Reactivating Invisible Backdoor Attacks

Although existing invisible backdoor attack methods overlook the impact of compression distortion on triggers, they have showcased the diversity of backdoor attack techniques. Different attacks have unique advantages and are suitable for different scenarios. Therefore, it is important to design a universal method to reactivate the failed trigger information in the binary bitstream $\hat{\mathbf{y}}$ of existing methods. This method relies on pixel-level ROI functionality and therefore applies only to LICs.

Based on the difference between the poisoned data and the original data, an intuitive idea is that the residuals between them are the crucial part of triggers. Thus, we first consider preserving more residual information in the $\hat{\mathbf{y}}$. To achieve this, we design the ROI mask \mathbf{M}_{res} to allocate more bits to areas with larger residuals, represented as follows

$$\mathbf{M}_{res} = \text{Norm}(\text{Mean}|\mathbf{x} - \mathbf{x}_p|),$$

where $\mathbf{x}_p \in \mathbb{R}^{3 \times H \times W}$ is a poisoned version of $\mathbf{x} \in \mathbb{R}^{3 \times H \times W}$ using previous attack methods, $\text{Mean}(\cdot)$ denotes averaging over the RGB channels, and $\text{Norm}(\mathbf{z}) = \frac{\mathbf{z} - \min(\mathbf{z})}{\max(\mathbf{z}) - \min(\mathbf{z})}$ is a normalization function. \mathbf{M}_{res} enables the decompressed poisoned image $\hat{\mathbf{x}}$ to preserve more details of the regions with high residuals.

However, we find that \mathbf{M}_{res} is not always the optimal solution. Inspired by Zeng *et al.* [28] and Rao *et al.* [29], we analyze which portions of the trigger information are significantly lost due to compression distortion. Since previously invisible triggers often introduce or change high-frequency components, the high-frequency components in the poisoned data likely are critical components of the trigger. As shown in the right of Fig. 1, removing these high-frequency components through Fast Fourier Transform during testing significantly decreases the attack success rate. Besides, image compression is much more influential to high-frequency components than to low-frequency information. Thus, the lossy compression compromises the trigger’s integrity, rendering it ineffective. Based on this insight, we aim to preserve the distribution and integrity of the high-frequency components in decompressed poisoned data $\hat{\mathbf{x}}$, which means that we need to reactivate the information of trigger’s high-frequency components in $\hat{\mathbf{y}}$.

To this end, we map the poisoned image \mathbf{x}_p to the frequency domain with the Fast Fourier Transform and extract the high-frequency components by a truncation function. These components contain crucial parts of the trigger and are highly susceptible to compression. Then, we use an inverse Fast Fourier transform to convert the high-frequency components back to the image domain and design a sample-specific ROI mask \mathbf{M}_{freq} according to the distribution of high-frequency components. By allocating more bitrate to these high-frequency components, we can mitigate their compression distortion and reactivate the ineffective triggers in the $\hat{\mathbf{x}}$. \mathbf{M}_{freq} is defined as

$$\mathbf{M}_{freq} = \text{Norm}(\text{Mean}|\mathcal{F}^{-1}(h_t(\mathcal{F}(\mathbf{x}_p)))|),$$

where \mathcal{F} is the Fast Fourier transform, and h_t denotes the truncation function at threshold t .

\mathbf{M}_{res} focuses more on preserving the residual areas, making it more effective for additive invisible triggers. In contrast, \mathbf{M}_{freq} protects the toxic high-frequency components, maintaining the trigger’s integrity during compression. The decompressed poisoned data $\hat{\mathbf{x}}_p$ can be expressed as follows, where \mathbf{M} is \mathbf{M}_{res} or \mathbf{M}_{freq} :

$$\hat{\mathbf{x}}_p = \text{Decoder}(\text{DeQ}(\text{Q}(\text{Encoder}(\mathbf{x}_p, \mathbf{M}))))).$$

It’s important to note that if there is a significant disparity in the compression distortion distribution between benign and poisoned samples after decompression, an additional trigger may be introduced. Therefore, for each benign sample \mathbf{x}_b , we randomly select a poisoned sample \mathbf{x}_p before compression and use its \mathbf{M}_{res} or \mathbf{M}_{freq} as the ROI mask of this benign sample, which preserves the characteristics of the original trigger. The decompressed benign data $\hat{\mathbf{x}}_p$ can be expressed as follows, where \mathbf{X}_p is the set of poisoned data before compression.

$$\hat{\mathbf{x}}_b = \text{Decoder}(\text{DeQ}(\text{Q}(\text{Encoder}(\mathbf{x}_b, \mathbf{M}(\mathbf{x}_p))))).$$

3.3 Compression-Adapted Attack (CAA)

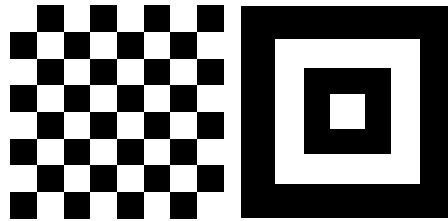
Departing from the technical route in Sec. 3.2, we propose a novel Compression-Adapted Attack (CAA) for data poisoning under lossy compression. The proposed attack applies to both LICs and traditional codecs with region-level ROI support.

Although changing the high-frequency components in previous attacks can ensure good invisibility, such alterations are not compression-friendly, which leads to the failure of invisible triggers after decompression. Unlike previous invisible attacks, we use the ROI to modify the high-frequency distribution, ensuring both invisibility and compression compatibility. Since regions with high ROI mask weights preserve more high-frequency details, while those with low weights suffer from greater high-frequency distortion, we can apply different ROI masks to poisoned and benign samples so that the decompressed poisoned and benign samples exhibit distinct high-frequency distributions.

We design a customized ROI mask M^* for all the samples to be poisoned. M^* guides specific compression that also affects \hat{y} . We use a uniformly distributed mask $M_{uniform}$ for all benign samples x_b , which compresses the image by assigning an equal bitrate to every region. Thus, the images with the customized ROI mask exhibit a certain frequency distribution after decompression, which serves as the trigger. This trigger ensures excellent invisibility. The decompressed poisoned data \hat{x}_p and the benign data \hat{x}_b can be expressed as:

$$\begin{aligned}\hat{x}_p &= \text{Decoder}(\text{DeQ}(\text{Q}(\text{Encoder}(x, M^*)))), \\ \hat{x}_b &= \text{Decoder}(\text{DeQ}(\text{Q}(\text{Encoder}(x_b, M_{uniform}))))).\end{aligned}$$

To enhance the resistant capabilities of our approach, we aim to ensure that customized spatial frequency distribution is global and repetitive [61]. We propose two specialized ROI mask options: 1. Checkerboard mask (Fig. 3a), and 2. Concentric square mask (Fig. 3b). The two ROI masks mentioned guide two distinct frequency distributions with adjustable density. The white areas, in comparison to the black areas, are allocated with higher bitrates, resulting in less distortion and better protection of high-frequency components. The specific high-frequency distributions of the decompressed poisoned samples are closely correlated with their corresponding masks. We encourage more interesting and effective designs for manipulated masks.



(a) Checkerboard (b) Concentric squares

Figure 3: Two options for ROI masks.

4 Experiments

4.1 Experimental Setting

Datasets. We evaluate backdoor attacks on three datasets including GTSRB [62], CIFAR-10 [63], and CelebA [64]. For the CelebA dataset, following [24, 22], we sample eight classes. We resize all images to 64×64 to match the mainstream image compression models and treat these images as raw images.

Evaluation Metrics. We evaluate the attacks using three metrics: Benign Accuracy (BA), Attack Success Rate (ASR) [65], and Attack Stealthiness (AS).

Classification Models. For our analysis, we employed four widely-used classification backbone models: ResNet-18 [66], Pre-activation ResNet-18 [67], MobileNet V2 [68] and SENet [69]. Optimization is performed using the Adam optimizer with an initial learning rate of 0.01, which is reduced by a factor of ten every 100 training epochs.

Codecs. We choose three classic LIC models, three traditional codec JPEG [57], BPG [58] and JPEG 2000 [60] that supports ROI for our experiments. The three LIC models Mbt-2018 [70], Cheng-2020 [47], and ELIC [53] have integrated ROI.

Baselines. We evaluate three classic invisible backdoor (WaNet [24], FTrojan [23], and BppAttack [22]) and two clean-label attacks (SAA [26] and Narcissus [27]) as baselines for our methods. We follow the default settings in their original papers and use the publicly available code from their official repositories for all experiments.

Backbone ↓	Dataset ↓	Method →	Clean	FTrojan	FTrojan _{ReA}	WaNet	WaNet _{ReA}	BppAttack	BppAttack _{ReA}	CAA
ResNet18	CIFAR-10	BA(%)	93.57	92.21	91.32(-0.89↓)	84.72	91.75(+7.03↑)	88.03	90.85 (+2.82↑)	93.28
		ASR(%)	-	12.53	94.91(+82.38↑)	77.58	98.43 (+20.85↑)	44.17	96.23 (+52.06↑)	100.00
	GTSRB	BA(%)	99.22	95.72	97.43(+1.71↑)	94.43	98.25 (+3.82↑)	90.78	94.84 (+4.06↑)	99.13
		ASR(%)	-	30.61	89.34(+58.73↑)	72.32	93.85 (+21.53↑)	42.25	87.23 (+44.98↑)	100.00
	CelebA	BA(%)	76.90	75.25	71.65(-3.60↓)	76.49	72.40 (-4.09↓)	74.69	71.58 (-3.11↓)	76.75
		ASR(%)	-	31.16	92.25(+61.09↑)	79.00	98.85 (+19.85↑)	32.73	95.97 (+63.24↑)	100.00
Pre-activation ResNet18	CIFAR-10	BA(%)	92.93	92.46	91.35(-1.11↓)	86.30	91.30 (+5.00↑)	90.61	90.59 (-0.02↓)	92.86
		ASR(%)	-	11.05	94.19(+83.14↑)	51.25	98.17 (+46.92↑)	16.17	95.03 (+78.86↑)	99.99
	GTSRB	BA(%)	99.13	94.25	97.02(+2.77↑)	92.73	97.43 (+4.70↑)	89.85	94.08 (+4.23↑)	99.13
		ASR(%)	-	23.26	83.77(+60.51↑)	71.80	92.26 (+20.46↑)	36.83	85.02 (+48.19↑)	99.95
	CelebA	BA(%)	76.78	74.98	70.34(-4.64↓)	76.55	74.83 (-1.72↓)	75.71	70.43 (-5.28↓)	76.57
		ASR(%)	-	27.37	92.91(+65.54↑)	88.87	95.45 (+6.58↑)	31.32	94.78 (+63.46↑)	99.93
MobileNetV2	CIFAR-10	BA(%)	92.58	91.86	90.64(-1.22↓)	90.35	90.65 (+0.30↑)	90.95	89.97 (-0.98↓)	92.43
		ASR(%)	-	10.71	91.58(+80.87↑)	16.74	96.37 (+79.63↑)	13.07	94.67 (+81.60↑)	99.99
	GTSRB	BA(%)	98.78	96.83	96.28(-0.55↓)	94.13	97.79 (+3.66↑)	95.97	93.82 (-2.15↓)	98.76
		ASR(%)	-	16.09	81.85(+65.76↑)	60.75	92.34 (+31.59↑)	22.75	78.28 (+55.53↑)	99.91
	CelebA	BA(%)	77.35	77.50	71.42(-6.08↓)	75.63	75.21 (-0.42↓)	77.51	71.73 (-5.78↓)	77.70
		ASR(%)	-	29.35	87.34(+57.99↑)	77.43	96.30 (+18.87↑)	31.91	90.92 (+59.01↑)	100.00
SENet	CIFAR-10	BA(%)	92.97	92.31	90.93(-1.38↓)	89.23	91.30 (+2.07↑)	90.67	91.15 (+0.48↑)	93.16
		ASR(%)	-	11.13	94.25(+83.12↑)	28.05	97.95 (+69.90↑)	16.14	96.03 (+79.89↑)	99.94
	GTSRB	BA(%)	98.75	94.87	97.17(+2.30↑)	95.02	97.69 (+2.67↑)	91.79	93.10 (+1.31↑)	98.69
		ASR(%)	-	29.68	87.43(+57.75↑)	63.25	92.70 (+29.45↑)	36.07	84.76 (+48.69↑)	99.89
	CelebA	BA(%)	77.10	74.73	71.71(-3.02↓)	76.49	72.10 (-4.39↓)	75.59	71.45 (-4.14↓)	77.06
		ASR(%)	-	30.21	91.58(+61.37↑)	79.00	96.78 (+17.78↑)	31.88	94.05 (+62.17↑)	99.46

Table 1: Comparison of different methods on multiple datasets.

4.2 Reactivating Ineffective Attacks

Ineffectiveness and reactivation. Tab. 1 presents the results in all-to-one attack mode of our Reactivation method and baselines. For all baselines and clean models (i.e., without backdoors), we use a uniformly distributed ROI mask $M_{uniform}$ to evaluate their performance under standard compression. For our Reactivation method, poisoned images are compressed with M_{freq} , while benign images are compressed using $M(x_p)$ defined in Sec. 3.2. All methods in Tab. 1 employ Mbt-2018 [70] with ROI, and we retain the poisoning rate from the baseline methods. Although all three methods achieve satisfactory BA and nearly 100% ASR in uncompressed settings [23, 22, 24], Tab. 1 reveals that inevitable compression in real-world application leads to a significant drop in both BA and ASR. WaNet achieves a higher ASR than FTrojan and BppAttack because its deformation-based triggers are less sensitive to compression. However, as shown in Fig. 1 and prior work [29], these deformations constitute only part of WaNet’s triggers, which also include compression-sensitive high-frequency components. Compression thus still degrades WaNet’s trigger integrity, while our reactivation approach significantly improves its ASR. These improvements in Tab. 1 highlight the effectiveness of our approach.

Reactivating ineffective clean-label attacks. Tab. 2 shows that clean-label attacks also easily fail under compression in real-world applications, which is because the adversarial perturbations these works introduced are compression-sensitive. We demonstrate the activation effect of our Reactivation method on two clean-label attacks (Sleeping Agent Attack (SAA) [26] and Narcissus [27]). These results further underscore the need to incorporate inevitable compression into data poisoning methods, and validate the effectiveness of our Reactivation method in clean-label attacks.

	SAA [26]	SAA _{ReA}	Narcissus [27]	Narcissus _{ReA}
BA	94.95	94.29	94.23	94.82
ASR	10.04	45.24	17.27	50.26

Table 2: Reactivating ineffective clean-label attacks.

Ablation studies of the ROI mask. To verify whether the ineffective triggers were successfully reactivated, we further evaluate the effectiveness of the ROI mask as shown in Tab. 3. First, we remove specific triggers from poisoned samples and compress them with M_{freq} , resulting in a significant drop in ASR. This shows the effective utilization of the original backdoor triggers. The non-zero attack performance is attributed to the high correlation between the frequency distribution of the trigger and the frequency masks. Second, applying a random binary ROI mask eliminates all

	Re-Activation	w/o Trigger	w/o Trigger & M_{freq}
FTrojan	83.77	42.13	0.43
WaNet	93.85	40.76	0.89
BppAttack	85.02	48.00	0.89

Table 3: Ablations for our Reactivation method.

	FTrojan	FTrojan _{ReA} -FFT	FTrojan _{ReA} -DCT	FTrojan _{ReA} -DWT
BA	87.73	86.80(-0.93)	86.92(-0.81)	87.35(-0.38)
ASR	34.77	92.17(+57.40)	91.87(+57.10)	90.87(+56.10)

Table 4: Impact of frequency decomposition.



Figure 4: **Visualization of the Reactivation Method.** Left: We provide the original images (without compression), decompressed images of three attack methods, their corresponding reactivated images, as well as the ROI mask.

trigger information, reducing ASR to nearly zero (Tab. 3), which verifies that our method reactivates original triggers rather than introducing new ones.

Ablation studies of frequency transformation. Tab. 4 shows the impact of different frequency-domain transformations used to compute M_{freq} on the results. The results are based on ResNet-18 and Mbt-2018, averaged across three datasets for comparison. Although FFT achieves a higher ASR, its BA is lower than that of DWT. Our goal is to extract trigger-relevant high-frequency components for mask design. Despite their differences, FFT, DCT, and DWT capture similar high-frequency signals, all suitable for our method, and all three frequency-domain variants of M_{freq} demonstrate strong attack-activation capability.

Stealthiness. As shown in Fig. 4, after compression, our method preserves the original attacks’ invisibility while reactivating ineffective triggers, without introducing visible artifacts. The visualization of M_{freq} shows that it is sample-specific and dependent on the activated attack.

4.3 Compression-Adapted Attack (CAA)

All-to-one attack. Tab. 1 presents the results of CAA in all-to-one attack mode. We utilize customized ROI mask M^* to compress the images to be poisoned, and $M_{uniform}$ to compress benign images. Our method achieves an average ASR of over 94.7% on all four backbone models across all datasets, while the BA performance was excellently maintained. The significant improvements in BA and ASR indicate that our method successfully implants a specific frequency distribution trigger.

All-to-all attack. To further demonstrate the robustness and generality of our method, we conduct an All-to-all experiment following previous approaches [8, 24, 22] in Tab. 5. In this experiment, ResNet18 served as the backbone. Our method outperforms alternatives across three datasets. Our CAA mislabels nearly 100% of poisoned images with only a 0.06% loss in BA. In contrast, baselines falter in all-to-all scenarios, suffering BA drops. These results underscore our method’s superiority.

Dataset	Method	Clean	FTrojan	WaNet	BppAttack	CAA
CIFAR-10	BA(%)	93.57	92.76	91.13	90.32	93.51
	ASR(%)	-	1.13	29.21	28.58	93.76
GTSRB	BA(%)	99.22	98.28	98.14	89.47	99.17
	ASR(%)	-	13.30	17.57	39.62	99.46
CelebA	BA(%)	76.90	75.50	76.66	73.03	76.85
	ASR(%)	-	3.50	55.57	19.17	76.77

Table 5: All-to-all attack result.

Performance on different compression models. We experiment with our Compression-Adapted attack using various LIC models [47, 53] and traditional model (JPEG [57], JPEG 2000 [60], BPG [58]) on CIFAR-10, as shown in Tab. 6. ResNet18 [66] is employed as the classification model. Our method consistently demonstrates minimal BA loss and high ASR close to 100% across different codecs. This performance underscores the broad applicability and generalizability of CAA. Please refer to the supplementary materials for additional results.

Codec	Method	Clean	FTrojan	WaNet	BppAttack	CAA
JPEG [57]	BA(%)	91.74	91.02	80.58	85.27	92.76
	ASR(%)	-	10.82	73.29	43.92	97.23
JPEG 2000 [60]	BA(%)	92.85	90.23	83.29	88.09	92.93
	ASR(%)	-	12.35	75.09	48.27	99.56
BPG [58]	BA(%)	93.58	92.10	90.55	92.48	92.39
	ASR(%)	-	13.07	76.97	44.97	100.00
Cheng-2020 [47]	BA(%)	93.21	91.34	84.86	88.25	93.14
	ASR(%)	-	11.89	77.32	43.73	100.00
ELIC [53]	BA(%)	93.79	92.32	85.22	87.35	93.53
	ASR(%)	-	12.64	78.32	46.73	99.77

Table 6: Performance on different codecs.

Resistance to defense methods.

We evaluate CAA method against the common defense methods, including Fine-Pruning [71], STRIP [72], and Gaussian noise and blur defenses. The introduction of defense methods is detailed in the supplementary material.

- The results of resisting Fine-Pruning are shown in Fig. 6, which indicate that Fine-Pruning cannot completely eliminate the backdoor implanted by our method. For instance, in the CIFAR-10 and GTSRB dataset, the ASR consistently exceeds the BA; in the CelebA dataset, the ASR achieves above 60%, showing that the backdoor is still effective.

- The results in Fig. 7 indicate that the entropy ranges of the clean model and the backdoored model trained on our poisoned samples, are very similar. Our method is resistant to STRIP in compression scenarios.

- After applying Gaussian blur (kernel:3) to decompressed test samples, we achieved a BA of 91.62% and an ASR of 98.72%. With Gaussian noise (std:1) added, BA was 86.86% and ASR reached 100%. These results demonstrate our method’s resilience against such defenses.

Robustness against re-compression. Tab. 7 reports the ASR under JPEG re-compression. As expected, FTrojan_{ReA} almost completely fails. Since FTrojan is not designed to be compression-adaptive, its trigger remains highly vulnerable to re-compression, even when it is injected before the initial compression stage. In contrast, the performance of CAA depends on both the re-compression quality factor and the selected ROI mask. When the JPEG quality factor is set to the default or a higher value, and a relatively sparse ROI mask is adopted, CAA consistently achieves an ASR above 95%. These results demonstrate that CAA offers substantially stronger robustness to practical re-compression than non-adaptive invisible attacks.

Comparisons of file sizes. Our method redistributes bits according to the ROI mask, assigning more bits to light (high-priority) regions while allocating fewer bits to dark regions. As a result, the overall bit allocation is adjusted spatially rather than uniformly increased. Consequently, the results in Tab. 8

Quality of Recompression	50 (low)	75 (default)	90 (high)
FTrojan _{ReA}	10.83	17.87	25.56
CAA (2×2 mask)	79.59	95.65	97.08
CAA (8×8 mask)	73.27	88.87	96.57

Table 7: ASR results of recompression with JPEG on GTSRB.

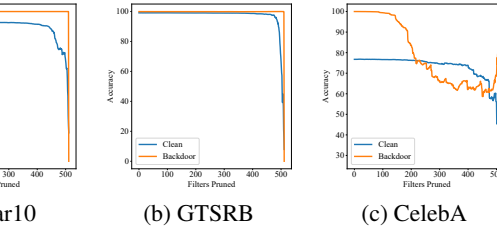


Figure 6: Resilient to Fine-Pruning [71]

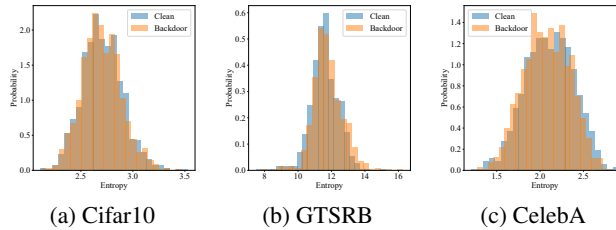


Figure 7: Resilient to STRIP [72]

	Std. Compression		FTrojan _{ReA}		CAA
Codec	ELIC	JPEG	ELIC	ELIC	JPEG
file size (KiB)	0.789	0.962	1.036	0.815	0.981
Bits (/pixel)	1.579	1.923	2.071	1.670	1.981

Table 8: Average file size (KiB) and bits (/pixel) on GTSRB.

show that our method does not noticeably increase file size, or equivalently, the resulting bit budget. This suggests that the improved attack effectiveness of our method is achieved with little additional storage or transmission overhead.

Stealthiness.

Fig. 8 is the visualization of CAA. (a) and (b) shows that poisoned images by CAA are visually imperceptible. As the ROI mask pattern becomes denser, stealth increases while attack performance remains unaffected. All reported experiments of CAA use an 8×8 checkerboard. Fig. 9 further analyzes our CAA method driven special frequency pattern: we split each image into four regions according to the ROI mask and show the DCT spectrum for each region. The poisoned images exhibit noticeably stronger high-frequency signals in the top-left and bottom-right regions than in the top-right and bottom-left. Such frequency pattern serves as a trigger correlated with the target class, enabling a successful backdoor.

Tab.9 shows that our method is imperceptible by both objective metrics and human perception (human inspection test setting follows WaNet [24]). Since prior invisible triggers fail under lossy compression, comparing stealth against those failed methods is meaningless; therefore we compare CAA with the visible attack BadNet [8]. Tab.9 demonstrates that CAA remains effective under lossy compression while offering superior stealth.

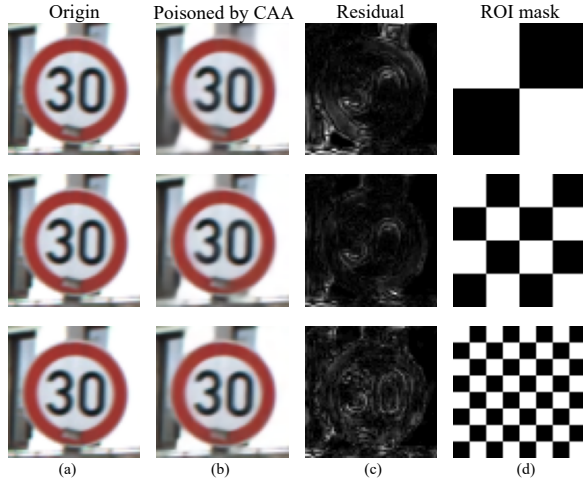


Figure 8: **Visualization of CAA.** (a) Origin images (without compression). (b) Poisoned images via CAA (all samples were classified as the target class). (c) The residuals. (d) The ROI masks.

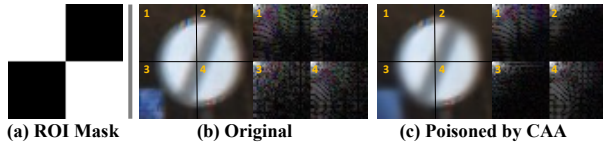


Figure 9: Frequency-Domain Visualization of CAA.

	PSNR \uparrow	SSIM \uparrow	Human Inspection Test \uparrow
No Attack	INF	1.000	-
BadNet	21.76	0.916	8.3
CAA	37.4	0.965	52.4

Table 9: Quantitative evaluation of stealthiness on CIFAR-10.

5 Conclusion and Future Work

In this paper, we address a key oversight in backdoor attack design by explicitly accounting for lossy data compression. We demonstrate that invisible backdoor attacks often become ineffective after compression. To overcome this challenge, we propose two ROI-based methods. Universal-Attack Activation generates sample-specific ROI masks to reactivate previously ineffective triggers while preserving attack diversity. Compression-Adapted Attack, in contrast, constructs new invisible triggers as frequency distributions that are inherently adapted to compression scenarios.

This work deepens the understanding of backdoor attacks under lossy compression. In future work, we will explore further optimizations and corresponding defenses. More importantly, our findings underscore the need to consider real-world data processing conditions when evaluating security vulnerabilities in deep learning systems. We hope this work will motivate future research on more practical attack and defense strategies.

References

- [1] Nicholas Carlini and David Wagner. Towards evaluating the robustness of neural networks. In *2017 IEEE Symposium on Security and Privacy (SP)*, pages 39–57. Ieee, 2017.
- [2] Qiuyu Duan, Zhongyun Hua, Qing Liao, Yushu Zhang, and Leo Yu Zhang. Conditional backdoor attack via jpeg compression. In *Proceedings of the AAAI Conference on Artificial Intelligence*, volume 38, pages 19823–19831, 2024.
- [3] Qian Li, Yuxiao Hu, Ye Liu, Dongxiao Zhang, Xin Jin, and Yuntian Chen. Discrete point-wise attack is not enough: Generalized manifold adversarial attack for face recognition. In *Proceedings of the IEEE/CVF Conference on Computer Vision and Pattern Recognition*, pages 20575–20584, 2023.
- [4] Robby Costales, Chengzhi Mao, Raphael Norwitz, Bryan Kim, and Junfeng Yang. Live trojan attacks on deep neural networks. In *Proceedings of the IEEE/CVF Conference on Computer Vision and Pattern Recognition Workshops*, pages 796–797, 2020.
- [5] Bao Gia Doan, Ehsan Abbasnejad, and Damith C Ranasinghe. Februus: Input purification defense against trojan attacks on deep neural network systems. In *Proceedings of the 36th Annual Computer Security Applications Conference*, pages 897–912, 2020.
- [6] Khoa Doan, Yingjie Lao, Weijie Zhao, and Ping Li. Lira: Learnable, imperceptible and robust backdoor attacks. In *Proceedings of the IEEE/CVF international conference on computer vision*, pages 11966–11976, 2021.
- [7] Jeremy Cohen, Elan Rosenfeld, and Zico Kolter. Certified adversarial robustness via randomized smoothing. In *international conference on machine learning*, pages 1310–1320. PMLR, 2019.
- [8] Tianyu Gu, Brendan Dolan-Gavitt, and Siddharth Garg. Badnets: Identifying vulnerabilities in the machine learning model supply chain. *arXiv preprint arXiv:1708.06733*, 2017.
- [9] Ingemar Cox, Matthew Miller, Jeffrey Bloom, Jessica Fridrich, and Ton Kalker. *Digital watermarking and steganography*. Morgan kaufmann, 2007.
- [10] Karan Ganju, Qi Wang, Wei Yang, Carl A Gunter, and Nikita Borisov. Property inference attacks on fully connected neural networks using permutation invariant representations. In *Proceedings of the 2018 ACM SIGSAC conference on computer and communications security*, pages 619–633, 2018.
- [11] Qian Li, Yuxiao Hu, Yinpeng Dong, Dongxiao Zhang, and Yuntian Chen. Focus on hidere: Exploring hidden threats for enhancing adversarial training. In *Proceedings of the IEEE/CVF Conference on Computer Vision and Pattern Recognition*, pages 24442–24451, 2024.
- [12] Yingqi Liu, Shiqing Ma, Yousra Aafer, Wen-Chuan Lee, Juan Zhai, Weihang Wang, and Xiangyu Zhang. Trojaning attack on neural networks. In *25th Annual Network And Distributed System Security Symposium (NDSS 2018)*. Internet Soc, 2018.
- [13] Yansong Gao, Change Xu, Derui Wang, Shiping Chen, Damith C Ranasinghe, and Surya Nepal. Strip: A defence against trojan attacks on deep neural networks. In *Proceedings of the 35th annual computer security applications conference*, pages 113–125, 2019.
- [14] Shaofeng Li, Minhui Xue, Benjamin Zi Hao Zhao, Haojin Zhu, and Xinpeng Zhang. Invisible backdoor attacks on deep neural networks via steganography and regularization. *IEEE Transactions on Dependable and Secure Computing*, 18(5):2088–2105, 2020.
- [15] Junyu Lin, Lei Xu, Yingqi Liu, and Xiangyu Zhang. Composite backdoor attack for deep neural network by mixing existing benign features. In *Proceedings of the 2020 ACM SIGSAC Conference on Computer and Communications Security*, pages 113–131, 2020.
- [16] Tuan Anh Nguyen and Anh Tran. Input-aware dynamic backdoor attack. *Advances in Neural Information Processing Systems*, 33:3454–3464, 2020.

- [17] Aniruddha Saha, Akshayvarun Subramanya, and Hamed Pirsiavash. Hidden trigger backdoor attacks. In *Proceedings of the AAAI conference on artificial intelligence*, volume 34, pages 11957–11965, 2020.
- [18] Ahmed Salem, Rui Wen, Michael Backes, Shiqing Ma, and Yang Zhang. Dynamic backdoor attacks against machine learning models. *EuroS&P 2022*, 2022.
- [19] Sonain Jamil, Md Jalil Piran, MuhibUr Rahman, and Oh-Jin Kwon. Learning-driven lossy image compression: A comprehensive survey. *Engineering Applications of Artificial Intelligence*, 123:106361, 2023.
- [20] Yueyu Hu, Wenhan Yang, Zhan Ma, and Jiaying Liu. Learning end-to-end lossy image compression: A benchmark. *IEEE Transactions on Pattern Analysis and Machine Intelligence*, 44(8):4194–4211, 2021.
- [21] Ruihan Yang and Stephan Mandt. Lossy image compression with conditional diffusion models. *Advances in Neural Information Processing Systems*, 36:64971–64995, 2023.
- [22] Zhenting Wang, Juan Zhai, and Shiqing Ma. Bppattack: Stealthy and efficient trojan attacks against deep neural networks via image quantization and contrastive adversarial learning. In *Proceedings of the IEEE/CVF Conference on Computer Vision and Pattern Recognition*, pages 15074–15084, 2022.
- [23] Tong Wang, Yuan Yao, Feng Xu, Shengwei An, Hanghang Tong, and Ting Wang. An invisible black-box backdoor attack through frequency domain. In *European Conference on Computer Vision*, pages 396–413. Springer, 2022.
- [24] Tuan Anh Nguyen and Anh Tuan Tran. Wanet-imperceptible warping-based backdoor attack. In *International Conference on Learning Representations*.
- [25] Yuezun Li, Yiming Li, Baoyuan Wu, Longkang Li, Ran He, and Siwei Lyu. Invisible backdoor attack with sample-specific triggers. In *Proceedings of the IEEE/CVF international conference on computer vision*, pages 16463–16472, 2021.
- [26] Hossein Souri, Liam Fowl, Rama Chellappa, Micah Goldblum, and Tom Goldstein. Sleeper agent: Scalable hidden trigger backdoors for neural networks trained from scratch. *Advances in Neural Information Processing Systems*, 35:19165–19178, 2022.
- [27] Yi Zeng, Minzhou Pan, Hoang Anh Just, Lingjuan Lyu, Meikang Qiu, and Ruoxi Jia. Narcissus: A practical clean-label backdoor attack with limited information. In *Proceedings of the 2023 ACM SIGSAC Conference on Computer and Communications Security*, pages 771–785, 2023.
- [28] Yi Zeng, Won Park, Z Morley Mao, and Ruoxi Jia. Rethinking the backdoor attacks’ triggers: A frequency perspective. In *Proceedings of the IEEE/CVF international conference on computer vision*, pages 16473–16481, 2021.
- [29] Quanrui Rao, Lin Wang, and Wuying Liu. Rethinking cnn’s generalization to backdoor attack from frequency domain. In *The Twelfth International Conference on Learning Representations*, 2024.
- [30] Joel Askelöf, Mathias Larsson Carlander, and Charilaos Christopoulos. Region of interest coding in jpeg 2000. *Signal Processing: Image Communication*, 17(1):105–111, 2002.
- [31] Myungseo Song, Jinyoung Choi, and Bohyung Han. Variable-rate deep image compression through spatially-adaptive feature transform. In *Proceedings of the IEEE/CVF international conference on computer vision*, pages 2380–2389, 2021.
- [32] Chunlei Cai, Li Chen, Xiaoyun Zhang, and Zhiyong Gao. End-to-end optimized roi image compression. *IEEE Transactions on Image Processing*, 29:3442–3457, 2019.
- [33] Yi Ma, Yongqi Zhai, Chunhui Yang, Jiayu Yang, Ruofan Wang, Jing Zhou, Kai Li, Ying Chen, and Ronggang Wang. Variable rate roi image compression optimized for visual quality. In *Proceedings of the IEEE/CVF Conference on Computer Vision and Pattern Recognition*, pages 1936–1940, 2021.

- [34] Hiroaki Akutsu and Takahiro Naruko. End-to-end learned roi image compression. In *CVPR Workshops*, page 0, 2019.
- [35] Yueqi Xie, Ka Leong Cheng, and Qifeng Chen. Enhanced invertible encoding for learned image compression. In *Proceedings of the 29th ACM international conference on multimedia*, pages 162–170, 2021.
- [36] Renjie Zou, Chunfeng Song, and Zhaoxiang Zhang. The devil is in the details: Window-based attention for image compression. In *Proceedings of the IEEE/CVF conference on computer vision and pattern recognition*, pages 17492–17501, 2022.
- [37] Jiahao Li, Bin Li, and Yan Lu. Hybrid spatial-temporal entropy modelling for neural video compression. In *Proceedings of the 30th ACM International Conference on Multimedia*, pages 1503–1511, 2022.
- [38] Yunuo Chen, Qian Li, Bing He, Donghui Feng, Ronghua Wu, Qi Wang, Li Song, Guo Lu, and Wenjun Zhang. S2cformer: Reorienting learned image compression from spatial interaction to channel aggregation. *arXiv preprint arXiv:2502.00700*, 2025.
- [39] Xinyun Chen, Chang Liu, Bo Li, Kimberly Lu, and Dawn Song. Targeted backdoor attacks on deep learning systems using data poisoning. *arXiv preprint arXiv:1712.05526*, 2017.
- [40] Yunfei Liu, Xingjun Ma, James Bailey, and Feng Lu. Reflection backdoor: A natural backdoor attack on deep neural networks. In *Computer Vision—ECCV 2020: 16th European Conference, Glasgow, UK, August 23–28, 2020, Proceedings, Part X 16*, pages 182–199. Springer, 2020.
- [41] Siyuan Cheng, Yingqi Liu, Shiqing Ma, and Xiangyu Zhang. Deep feature space trojan attack of neural networks by controlled detoxification. In *Proceedings of the AAAI Conference on Artificial Intelligence*, volume 35, pages 1148–1156, 2021.
- [42] Yuezun Li, Yiming Li, Baoyuan Wu, Longkang Li, Ran He, and Siwei Lyu. Invisible backdoor attack with sample-specific triggers. In *Proceedings of the IEEE/CVF international conference on computer vision*, pages 16463–16472, 2021.
- [43] Aniruddha Saha, Akshayvarun Subramanya, and Hamed Pirsiavash. Hidden trigger backdoor attacks. In *Proceedings of the AAAI conference on artificial intelligence*, volume 34, pages 11957–11965, 2020.
- [44] Alexander Turner, Dimitris Tsipras, and Aleksander Madry. Label-consistent backdoor attacks. *arXiv preprint arXiv:1912.02771*, 2019.
- [45] Johannes Ballé, Valero Laparra, and Eero P Simoncelli. End-to-end optimized image compression. In *5th International Conference on Learning Representations, ICLR 2017*, 2017.
- [46] Johannes Ballé, David Minnen, Saurabh Singh, Sung Jin Hwang, and Nick Johnston. Variational image compression with a scale hyperprior. In *International Conference on Learning Representations*, 2018.
- [47] Zhengxue Cheng, Heming Sun, Masaru Takeuchi, and Jiro Katto. Learned image compression with discretized gaussian mixture likelihoods and attention modules. In *Proceedings of the IEEE/CVF conference on computer vision and pattern recognition*, pages 7939–7948, 2020.
- [48] Fangdong Chen, Yumeng Xu, and Li Wang. Two-stage octave residual network for end-to-end image compression. In *Proceedings of the AAAI Conference on Artificial Intelligence*, volume 36, pages 3922–3929, 2022.
- [49] Yin hao Zhu, Yang Yang, and Taco Cohen. Transformer-based transform coding. In *International Conference on Learning Representations*, 2022.
- [50] Jinming Liu, Heming Sun, and Jiro Katto. Learned image compression with mixed transformer-cnn architectures. In *Proceedings of the IEEE/CVF conference on computer vision and pattern recognition*, pages 14388–14397, 2023.

- [51] Yunuo Chen, Zezheng Lyu, Bing He, Hongwei Hu, Qi Wang, Yuan Tian, Li Song, Wenjun Zhang, and Guo Lu. Content-aware mamba for learned image compression. In *The Fourteenth International Conference on Learning Representations*, 2026.
- [52] Yiwei Zhang, Guo Lu, Yunuo Chen, Shen Wang, Yibo Shi, Jing Wang, and Li Song. Neural rate control for learned video compression. In *The Twelfth International Conference on Learning Representations*, 2023.
- [53] Dailan He, Ziming Yang, Weikun Peng, Rui Ma, Hongwei Qin, and Yan Wang. Elic: Efficient learned image compression with unevenly grouped space-channel contextual adaptive coding. In *Proceedings of the IEEE/CVF Conference on Computer Vision and Pattern Recognition*, pages 5718–5727, 2022.
- [54] Dailan He, Yaoyan Zheng, Baocheng Sun, Yan Wang, and Hongwei Qin. Checkerboard context model for efficient learned image compression. In *Proceedings of the IEEE/CVF Conference on Computer Vision and Pattern Recognition*, pages 14771–14780, 2021.
- [55] David Minnen and Saurabh Singh. Channel-wise autoregressive entropy models for learned image compression. In *2020 IEEE International Conference on Image Processing (ICIP)*, pages 3339–3343. IEEE, 2020.
- [56] Yichen Qian, Xiuyu Sun, Ming Lin, Zhiyu Tan, and Rong Jin. Entroformer: A transformer-based entropy model for learned image compression. In *International Conference on Learning Representations*.
- [57] David Bařina and Ondřej Klřma. Region of interest in jpeg. pages 1–5, 01 2022.
- [58] David Yee, Sara Soltaninejad, Deborsi Hazarika, Gaylord Mbuyi, Rishi Barnwal, and Anup Basu. Medical image compression based on region of interest using better portable graphics (bpg). In *2017 IEEE international conference on systems, man, and cybernetics (SMC)*, pages 216–221. IEEE, 2017.
- [59] Andrew P Bradley and Fred WM Stentiford. Jpeg 2000 and region of interest coding. In *Digital Image Computing Techniques and Applications*, volume 2, pages 1–6. Citeseer, 2002.
- [60] Athanassios Skodras, Charilaos Christopoulos, and Touradj Ebrahimi. The jpeg 2000 still image compression standard. *IEEE Signal processing magazine*, 18(5):36–58, 2001.
- [61] Changjiang Li, Ren Pang, Zhaohan Xi, Tianyu Du, Shouling Ji, Yuan Yao, and Ting Wang. An embarrassingly simple backdoor attack on self-supervised learning. In *Proceedings of the IEEE/CVF International Conference on Computer Vision*, pages 4367–4378, 2023.
- [62] Johannes Stalkamp, Marc Schlipf, Jan Salmen, and Christian Igel. Man vs. computer: Benchmarking machine learning algorithms for traffic sign recognition. *Neural networks*, 32:323–332, 2012.
- [63] Alex Krizhevsky, Geoffrey Hinton, et al. Learning multiple layers of features from tiny images. 2009.
- [64] Ziwei Liu, Ping Luo, Xiaogang Wang, and Xiaoou Tang. Deep learning face attributes in the wild. In *Proceedings of the IEEE international conference on computer vision*, pages 3730–3738, 2015.
- [65] Akshaj Kumar Veldanda, Kang Liu, Benjamin Tan, Prashanth Krishnamurthy, Farshad Khorrani, Ramesh Karri, Brendan Dolan-Gavitt, and Siddharth Garg. Nnucleation: broad spectrum and targeted treatment of backdoored dnns. *arXiv preprint arXiv:2002.08313*, 3:18, 2020.
- [66] Kaiming He, Xiangyu Zhang, Shaoqing Ren, and Jian Sun. Deep residual learning for image recognition. In *Proceedings of the IEEE conference on computer vision and pattern recognition*, pages 770–778, 2016.
- [67] Kaiming He, Xiangyu Zhang, Shaoqing Ren, and Jian Sun. Identity mappings in deep residual networks. In *Computer Vision–ECCV 2016: 14th European Conference, Amsterdam, The Netherlands, October 11–14, 2016, Proceedings, Part IV 14*, pages 630–645. Springer, 2016.

- [68] Mark Sandler, Andrew Howard, Menglong Zhu, Andrey Zhmoginov, and Liang-Chieh Chen. Mobilenetv2: Inverted residuals and linear bottlenecks. In *Proceedings of the IEEE conference on computer vision and pattern recognition*, pages 4510–4520, 2018.
- [69] Jie Hu, Li Shen, and Gang Sun. Squeeze-and-excitation networks. In *Proceedings of the IEEE conference on computer vision and pattern recognition*, pages 7132–7141, 2018.
- [70] David Minnen, Johannes Ballé, and George D Toderici. Joint autoregressive and hierarchical priors for learned image compression. *Advances in neural information processing systems*, 31, 2018.
- [71] Kang Liu, Brendan Dolan-Gavitt, and Siddharth Garg. Fine-pruning: Defending against backdooring attacks on deep neural networks. In *International symposium on research in attacks, intrusions, and defenses*, pages 273–294. Springer, 2018.
- [72] Yansong Gao, Change Xu, Derui Wang, Shiping Chen, Damith C Ranasinghe, and Surya Nepal. Strip: A defence against trojan attacks on deep neural networks. In *Proceedings of the 35th annual computer security applications conference*, pages 113–125, 2019.